

# Supporting Information

Tomasi and Volkow 10.1073/pnas.1001414107

## SI Results

### Variability of the IFCD Strength of the Hubs Across Research Sites.

Using ROI analyses we confirmed that the posterior cingulate/ventral precuneus cluster was the most prominent hub for 18 of the 22 research sites in this study. For the MIT dataset, however, the posterior cingulate/ventral precuneus did not include a prominent functional hub (i.e.,  $k$  was 45% lower for this region than for the

cuneus). Only 4 research sites (MIT, New York B, Ontario, and Orangeburg) had their most prominent hubs in brain regions other than the posterior cingulate/ventral precuneus (MIT, cuneus, BA 18, left and right; Orangeburg and New York B, cingulate cortex; Ontario, cerebellum, fastigium). For these datasets, the  $k_{\max}$  was up to 20%  $>k$  in posterior cingulate/ventral precuneus. Overall, parietal, occipital, and posterior limbic regions had higher IFCD.

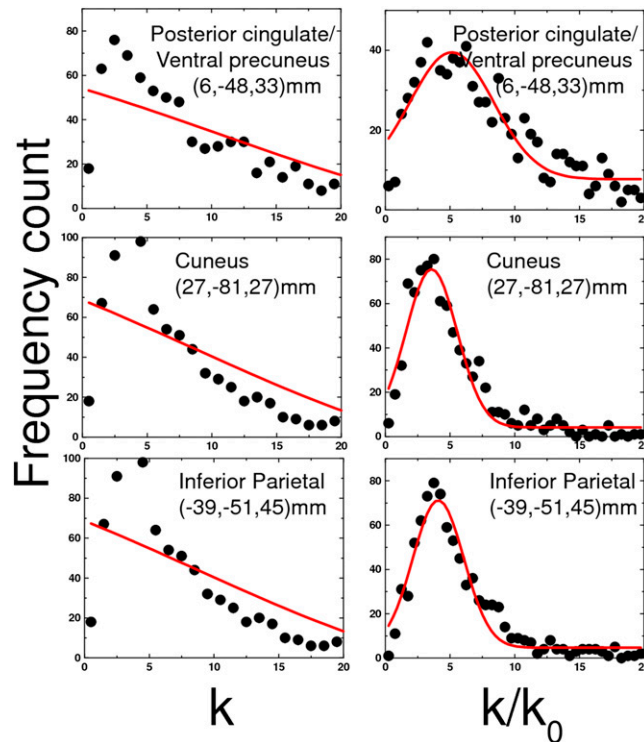


**Fig. S1.** Distribution of the absolute ( $k$ , *Left*) and rescaled ( $k/k_0$ , *Right*) IFCD across subjects (black circles) in three different 9-mm isotropic cubic ROIs at the locations of main functional connectivity hubs (Table 1) and the corresponding Gaussian curve fit (red curves). The Gaussian curve failed to fit the distribution of the IFCD (*Left*) because of the large variability of the data across research sites, which might reflect differences in MRI hardware (magnetic field strength, coils, etc.) and software (pulse sequence, repetition time, echo time, reconstruction, etc.). The use of the normalization factor,  $1/k_0$ , reflecting the mean IFCD across subjects and voxels in the brain,  $k_0$ , allowed us to normalize the distribution of the IFCD (*Right*). Data from 979 healthy subjects are shown.

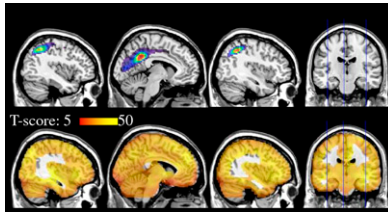


Fig. S2. Distribution of the rescaled IFCD,  $k/k_0$ , showing the main functional connectivity hubs in the brain (Upper) and the statistical significance of the rescaled IFCD (Lower) across 979 subjects, superimposed on sagittal MRI views of the human brain. Statistical significance threshold:  $P < 0.05$ , corrected for multiple comparisons (FWE).

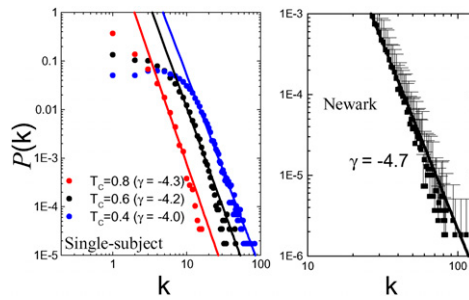


Fig. S3. Probability distribution of the IFCD in the human brain for a typical subject of the Newark dataset and three different  $T_c$  criteria (Left) and for a group of 19 healthy subjects of the same dataset ( $T_c = 0.6$ , Right) as a function of the number of functional connections per voxel,  $k$ , exemplifying the power scaling,  $P(k) = k^\gamma$ , of the IFCD.

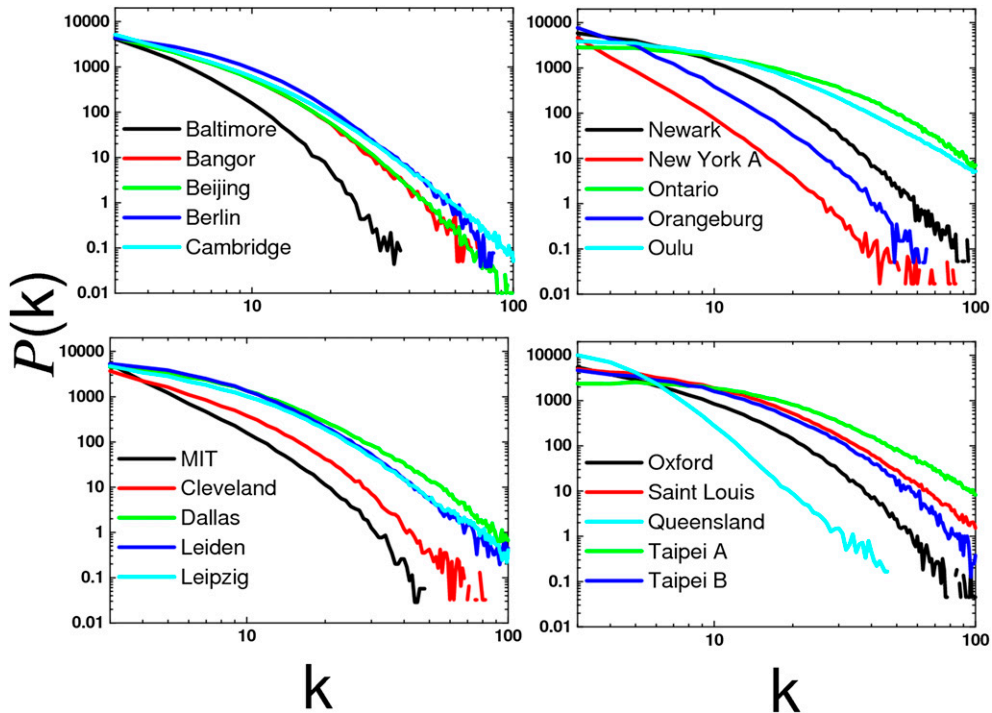


Fig. S4. IFCD probability distribution,  $P(k) = n(k)/n_0$ , reflecting the ratio between the average number of voxels,  $n(k)$ , with  $k$  functional connections and the total number of voxels in the brain,  $n_0$ , as a function of  $k$  for each research site in the study (Table 2).





*Resting-state imaging time series*



*Image realignment*



*Spatial Normalization*



*Motion filtering*



*Physiologic noise filtering*



*Temporal filtering*



*FCD Estimation*



*Spatial smoothing*



*Statistical analysis*

Fig. S8. Flow diagram for FCDM.